Hindawi
Advances in Materials Science and Engineering
Volume 2023, Article ID 1524836, 11 pages
https://doi.org/10.1155/2023/1524836

Research Article

Effects of Predefined Thermomechanical Procedure on the Microstructure and Mechanical Properties of the Two-Way Shape Memory Effect in the NiTi Alloy

Ali Tahaei,[1] **Ali Aghajani**,[1] **Mahmoud Abbasi**,[2] **Behrouz Bagheri**,[2] **Mattia Merlin**,[3] **and Gian Luca Garagnani**[3]

[1]*Kharazmi University, Tehran, Iran*
[2]*Amirkabir University of Technology, Tehran, Iran*
[3]*University of Ferrara, Ferrara, Italy*

Correspondence should be addressed to Ali Aghajani; aghajani_a@yahoo.com

Received 22 November 2022; Revised 8 April 2023; Accepted 20 May 2023; Published 7 June 2023

Academic Editor: Sachin Salunkhe

In the current paper, a predefined thermomechanical procedure has been applied to the two-way shape memory effect (TWSME) in a NiTi alloy to study the effect of two different applied load conditions on the induced martensitic state. The microstructure of the strips was studied using optical microscopy (OM), scanning electron microscopy (SEM) fitted with an EDS microprobe, and microhardness tests at the end of both the training and thermal cycles. Inducing internal stresses along specified directions during training cycles results in the formation of oriented martensitic variants rather than expected twinned martensitic variants upon cooling. It was found that the microstructure is made up of interlocking martensitic lathes, including the fine martensite colony next to the coarse martensite lathes. Furthermore, the results of the average hardness tests for bending at one point and three points were 241 and 247 HV0.2, respectively. It was shown that only the cubic austenitic phase (B2) and the martensitic monoclinic phase (B19′) experience transformation. The results reveal that homogeneous bending in three locations leads to achieving the best difference between high- and low-temperature curvatures after training.

1. Introduction

Due to their combination of the shape memory effect (SME), superelasticity, biocompatibility, and high reliability, shape memory alloys (SMAs), particularly NiTi alloys, are regarded as smart materials for the development of new advanced devices [1]. These materials are characterized by the presence of two different phases, namely, austenite, stable at high temperatures, and martensite, stable at low temperatures [2]. The shape memory effect is caused by the thermo-elastic martensitic transformation and the corresponding shape changes in the crystallographic lattice. The shape memory effect should be improved by carefully studying and optimizing the chemical composition, annealing, and shape-setting treatments [3]. There are four transformation temperatures present in shape memory alloys. During cooling, austenite undergoes a forward transformation into martensite, which starts at the martensitic start temperature (Ms) and ends at the martensitic finish temperature (Mf). When heated, martensite undergoes a reverse transformation into austenite that starts at the austenitic start temperature (As) and ends at the austenitic finish temperature (Af) [4]. These transformation temperatures range from absolute zero to around 100°C and are therefore suitable for a variety of near-ambient temperature applications.

Numerous mechanical devices that rely on NiTi wires or strips to induce a particular actuation use the one-way shape memory effect (OWSME). This effect is the material's capacity to recover significantly from large deformations experienced during heating above a critical temperature. The OWSME has found uses in various applications, such as

automotive, aerospace, biomedical, and civil engineering, because it can allow for a device to be stored and applied in a compacted deformed martensite state and then deployed through recovery into its original shape by undergoing a thermal transformation into the austenite phase [5]. However, the OWSME is limited in applications, as it can only recover once via a transformation from the deformed martensite phase into the austenite phase; upon return cooling into the martensitic phase after deployment, the material will maintain the deployed shape.

In addition to the one-way shape memory effect (OWSME), the NiTi alloys may also exhibit the two-way shape memory effect (TWSME). In the absence of applied stress, the material exhibits a return to the reoriented martensitic shape upon cooling below Ms. An internal elastic stress is created inside the material during the training process by applying deformation that is greater than the plastic range. Altering the thermal cycles causes the material to take on various shapes [6]. By creating an internal elastic stress field in the shape memory alloys, prior researchers [7] have experimented with various training techniques to achieve the two-way shape memory effect (TWSME). Some of the typical two-way training methods fall into the following categories [8]:

(1) Significant deformation caused by cooling below the Martensite finish temperature

(2) Deforming and heating above Austenite finish temperature while cooling below Martensite finish temperature

(3) Loading and unloading and cooling below M_d

(4) Cooling below Martensite finish temperature, loading and constraint, release, and heating above Austenite finish

(5) Heat above the Austenite finish, deforming and constraining, cooling below the Martensite finish, and cycling between these two finishes

Ponikarova et al. [9] investigated the two-way shape memory effect degradation due to stress relaxation during holding predeformed Ni-50.0 at % Ti alloy at temperatures from a range of 640–700 K for 0–60 min. They found that the main degradation of the two-way shape memory effect is related to holding the sample up to 60 min, while full degradation is not observed even after holding at 700 K for 6 h. A three-dimensional finite strain constitutive model for SMAs was applied by Xu et al. [10] to investigate the two-way shape memory effect through a large deformation framework. It was reported that the model is capable of predicting the TWSME for thermos-mechanically trained SMAs under load-free conditions and also capturing the decreasing stress level to initiate the phase transformation during pseudoelastic cycling by application of an accumulating internal stress tensor. Rita et al. [11] studied the thermomechanical treatment to achieve stable two-way shape memory strain. They showed that the TWSME can be achieved in the Ti-49.8 at.% Ni alloy by rolling to 40% thickness reduction in austenite phase at temperatures 470–870 K due to the formation of anisotropic internal stress fields and, at the same time, the recrystallization and recovery process of grains for rolling under high temperature.

As a result of the martensite phase change, anisotropic dislocations develop inside the matrix. Due to the anisotropic stress field created by these dislocations, martensite with preferentially oriented variance can be formed. Therefore, the macrostructure evolves during thermal cycles. Previous research on TWSME focused on the generation, explanation, and impact of various parameters on the magnitude of this effect [12, 13]. Additionally, the impact of applying various prestrains and deformation was previously investigated on various NiTi alloy types with the addition of third alloy elements [14–17]. Qader et al. [18] studied the effect of boron elements on microstructure evolution and thermomechanical properties of a Ni-riched NiTi shape memory alloy. It was found that the biocompatibility of NiTi alloy was improved by adding only 0.8 at % B due to a reduction in Ni ion release. The effect of Ta content on thermomechanical properties and transformation temperature of shape memory NiTi alloys was investigated by Dagdelen et al. [19]. They found that by increasing the amount of Ta, the dendrites' length of microstructure increased while random orientations decrease. In addition, as the amount of Ta increased, the phase transformation temperatures of the specimens significantly changed. The influence of Zr on microstructure and mechanical properties of shape memory alloys was investigated by Li et al. [20]. It was concluded that the transformation temperatures decreased linearly in approximately with the Zr content increasing up to 5 at. %. Moreover, the Zr addition led to the reduction of the size of the Ti_2Ni type second phase, and the critical stress for the martensite reorientation and the tensile strength were significantly improved.

Despite extensive research, according to the authors' knowledge, there is still a lack of knowledge regarding the best way to maximize the two-way shape memory effect. Common methods generally involve deforming the material while it is in the martensitic phase, heating it to a temperature above austenite's melting point, and then cooling it below martensite's point. Due to this, the goal of the current study is to alter the deformation strain during the training procedure by applying bending deformation at the strip's center at one point (BD1P) and three points (BD3P). The obtained results revealed that the bent sample had a stable and maximum two-way shape memory effect.

2. Experimental Procedure

In this study, Memory Alloy Co. provided nearly equiatomic NiTi plates (50.2% Ni–49.8% Ti). The strips were then cut from the plates using electro-discharge machining (EDM), having dimensions of 50, 3, and 1.52 mm. Prior to the shape-memorizing heat treatment, all specimens underwent annealing treatment by being heated to 750°C for 25 minutes in an electric furnace to undo any prior treatments. Flat shape strips were taken into consideration for memorization. After 25 minutes at 500°C in the furnace, the strips were removed and cooled in a glycol bath (–15°C). By experimenting with various time and temperature combinations

to find the ideal parameters, the time and temperature of the shape-memorizing treatment were determined from earlier studies [21].

Differential scanning calorimetry (DSC) was used to analyze the material's transformation behavior and determine the precise Martensite and Austenite start and finish temperatures by preparing a sample with a weight of 10 mg and a size of less than 4 mm and a constant heating/cooling rate of 10 C/min.

2.1. Training. According to previous research, 10–15% deformation was recommended for the strip to achieve the maximum two-way shape memory effect [22]. Another study that used a bending strain of 7% for training produced poor and unstable TWSME of less than 1% [2]. Additionally, applying a load that is over 15% has the opposite effect. Therefore, 12% strain deformation was chosen for the strips in this study and applied. The following steps were repeated for a specific number of cycles before being applied to the strips as part of a specially designed training process:

(1) Prestrain in a glycol bath with uniform bending at $T > M_f$

(2) Heating in hot water at $T > A_f$

(3) Cooling in the glycol bath at $T > M_f$ (–15°C)

Based on selecting the 12% strain for the primary deformation of TWSME, the necessary diameter of the bending mandrel was calculated based on the following equation:

$$\varepsilon_{\mathrm{d}} = \frac{\mathrm{d}}{(\mathrm{d} + 2R)}, \tag{1}$$

which ε_d is the applied strain, d is the thickness of the strip, and R is radius of the bending mandrel.

As a result, a mandrel with a diameter of 11.15 mm was considered for bending. Figure 1 indicates the schematic form of two-way strain during the training procedure. The strain of each sample in hot and cold positions was calculated by the following equation:

$$\varepsilon_{\mathrm{hot/cold}} = \left(\frac{\mathrm{d}}{2}\right) \times \left(\mathrm{curvature}_{\mathrm{hot/cold}}\right), \tag{2}$$

and then two-way strain was calculated by differences of strain in hot and cold positions according to the following equation:

$$\varepsilon_{tw} = \varepsilon_{\mathrm{cold}} - \varepsilon_{\mathrm{hot}}. \tag{3}$$

A specially created tool was used to apply the prestrain in each and every strip. The external layers of the strips could be subjected to a strain of up to 12% using this tool. Twenty times, the load application, heating, and cooling processes were repeated. Each stage of the ensuing strain analysis procedure involved taking an image of the strips. The strips were then put through several thermal cycles to see if the material could remember both low-temperature and high-temperature shapes. To freeze the position of each step, an image of the strip in the heating and cooling positions was taken using the same camera, objective distance, and magnification. Using commercial image analyzer software, the obtained images were examined to determine the curvature of the strip in each step. The schematic of the experimental setup for the training procedure is shown in Figure 2.

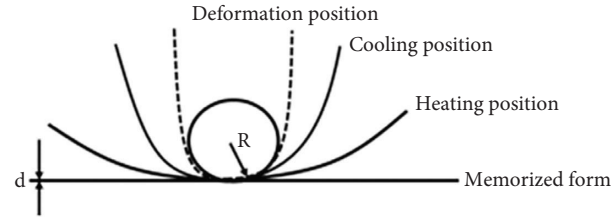

Figure 1: Schematic form of two-way shape memory effect during training.

2.2. Metallography and Microhardness. For mounting, the sample was cut by EDM into small dimensions. To achieve the mirror surface, the samples were ground with emery papers ranging in size from 400 to 2500 and then polished with 6-, 3-, and 1-micron alumina. The samples' microstructure was examined using an etchant made of HFHNO$_3$-CH$_3$COOH [14]. In order to study the microstructural changes brought on by training, microstructural analysis was also carried out using optical microscopy (OM) and scanning electron microscopy (SEM) Zeiss EVO MA 15 equipped with an EDX microprobe. According to standard UNI EN 6507 : 2006, a 200 gf load was applied to each sample for 15 seconds during the hardness test, and eight points through the thickness were measured.

2.3. X-Ray Diffraction. X-ray diffraction is a valuable tool for determining the crystallographic structure of materials. For detection of the existing phases, X-ray diffraction was performed on BD1P, BD3P, and as-received strip. The Brucker AXS D-8 XRD equipment was applied using CuKα radiation ($\lambda = 0.154$ nm) at 40 kv and 20 mA. The XRD spectra of the specimen were recorded in the 2θ range between 8 and 120° with a scan step of 0.01°.

3. Results and Discussion

3.1. DSC Results. Differential scanning calorimetry (DSC) was performed on the sample to determine the transformation temperature of the strip. The DSC results demonstrated the importance of austenite start and finish (A_s, A_f) and martensite start and finish (M_s, M_f) for the form strip that had been memorized and received. The transformation peak at higher temperatures is related to the martensite to austenite (B19′–B2) phase transformation while the peak at lower temperatures stems from the austenite to martensite (B2–B19′) phase transformation. The tangent line between the peaks on the DSC curves was used to calculate this value. It should be noted that precise temperature measurement was challenging due to the

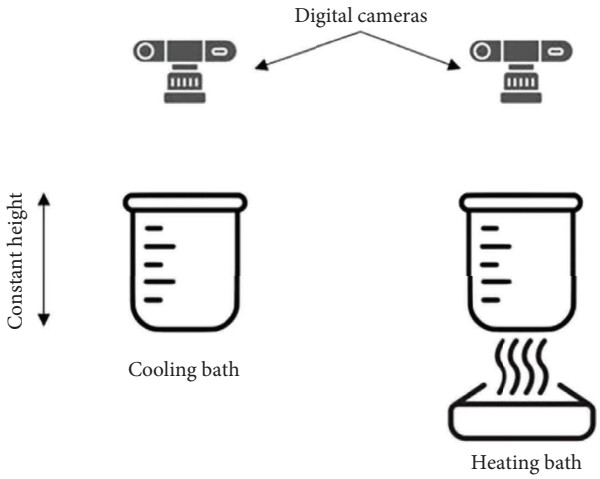

Figure 2: Schematics of the experimental test setup.

peculiar shape of DSC curves. Additionally, Table 1 categorizes all pertinent temperature information.

According to the DSC results, only the cubic austenitic phase (B2) and the martensitic monoclinic phase (B19′) underwent a transformation. According to one study, the chemical composition of the alloy and previous cold working has a significant impact on transformation temperatures [23]. Additionally, as shown in Figure 3, the application of the shape-memorizing heat treatment has changed the transformation temperatures. According to Kaya et al. [23], solutionized $Ni_{50.8}Ti_{49.02}$ alloys could show positive and negative TWSME if they are plastically deformed in martensite and austenite (above M_d), respectively.

3.2. Microstructural Analysis. Grain size is one of the most significant microscopic parameters of polycrystalline materials, which can observably impact mechanical behavior. For NiTi SMAs, a lot of research studies on the mechanical properties of such alloys with grain size have been reported [24–26]. It has been indicated that the tensile strength and Young's modulus of NiTi SMAs both increase by reducing the grain size due to the inhibition of stress-induced martensite transformation in the ultrafine grains. Martensite dominated the microstructure in this study. Following thermal cycles, Figure 4 shows optical microscopy of both strips of NiTi alloy. As is evident, the microstructure is made up of interlocking martensitic lathes (needles with various sizes and oriented directions). Additionally, the fine martensite colony can be seen next to the coarse martensite lathes. The SEM images of both samples taken at the edge and center of the strips are shown in Figures 5 and 6, respectively. It is known that a decrease in grain size depresses the martensitic transformation which is the reason for the unique functional properties of shape memory alloys and significantly influences the martensite twin structure [27]. To be more specific, as reducing the grain size, the plastic deformation resistances gradually increase due to the Hall-Patch effect, and the grain size effect of martensite transformation and reorientation reduces the deformation mismatch introduced in the polycrystalline system and leads to the decrease of local internal stress level during the cyclic deformation; therefore, the generation and accumulation of plastic deformation are inhibited [28].

Table 1: Transformation temperature of the sample.

	M_r	M_s	A_s	A_f
As-received	−19.6	51.0	13.3	111.7
Memorized shape	−13.3	43.7	19.6	100.6

The sample's EDS analysis, which revealed the alloy's elemental composition in percentage terms, is shown in Figure 7. Figure 8 also shows the strip's distribution map for the elements nickel and titanium as well as the high homogeneity of the element distribution in the microstructure.

3.3. Microhardness Test. When comparing shape memory alloys to conventional materials, measuring the mechanical properties such as hardness revealed significant differences due to phase deformation and changing phase volume during heating and cooling stages. This is primarily caused by the intrinsic properties' contribution of interface energy and bulk phase transition energy [29]. The resistance to deformation caused by dislocation motion and martensite reorientation can affect how hard NiTi shape memory alloys are.

The hardness profile for each sample is drawn in Figure 9. For BD1P, the hardness is comparatively higher on the external and internal surfaces of the thickness than in the center. The outer and inner parts of the strips are put under tension and compression, respectively, when they are bent into a round shape. Work hardening, which results from the material's deformation during repeated bending and ultimately increases hardness, happens as a result. Moreover, it is possible to say that dislocations reach that zone's precipitation and accumulate there. In BD3P, the value of hardness is essentially constant throughout the thickness, in contrast to BD1P. The most common deformation mode in bending is slip along slip bands that are evenly spaced close to the neutral axis. In order to leave traces on deformed specimens, slip tends to concentrate on a small subset of all possible slip planes. More slip bands form through the thickness and dislocations are more evenly distributed in the sample BD3P, which causes the hardness value to essentially hold steady. Furthermore, the results of the average hardness tests for bending at one point and three points were 241 and 247 HV0.2, respectively, which are largely comparable.

Two parallel deformation mechanisms that act during the training cycles are twining and slipping of the dislocations. Twins become larger under cyclic loading, and dislocations caused by shearing allow precipitation to move more quickly. These two mechanisms cause the hardness to increase, especially near surfaces. This work can be compared to Gloanec et al.'s [30] investigation of the low cycle fatigue behavior of NiTi alloys. After each cycle, they noticed an increase in the dislocation density. They discovered a large number of microtwins. Additionally, they discovered that the dislocations shear precipitates. Due to the small number of training cycles used in this study, some

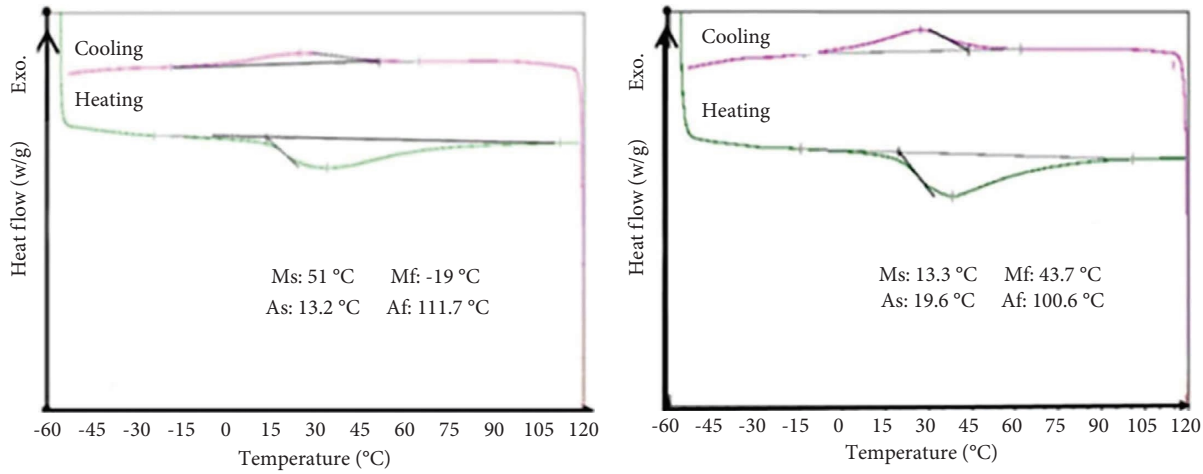

Figure 3: Transformation temperatures of the alloy specimen (DSC): (a) as-received (b) and memorized shape.

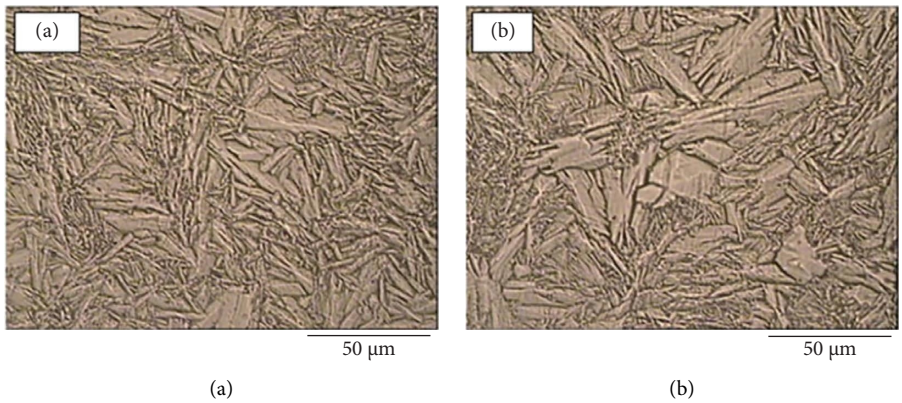

Figure 4: Microstructure of NiTi alloy with optical microscope: (a) BD1P and (b) BD3P.

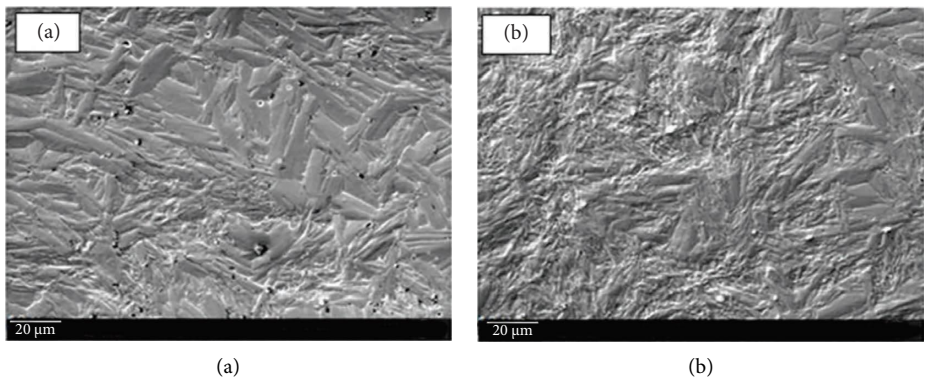

Figure 5: (a) BD1P and (b) BD3P nondeformed part.

precipitates are still not completely shorn by dislocations. As a result, a portion of the material retains the precipitates, such as no cycled material.

First, oriented martensite variants form during bending deformation and training and then dislocation generation occurs. Dislocations in the base material and martensite variants are of the same nature. There are also two mechanisms for the dislocations to slip and twine. Twins become loggers in cyclic loading, and dislocations with shearing the precipitates can slip more quickly. The pre-existing martensite underwent a reverse transformation during heating, and the elongated martensite underwent a significant

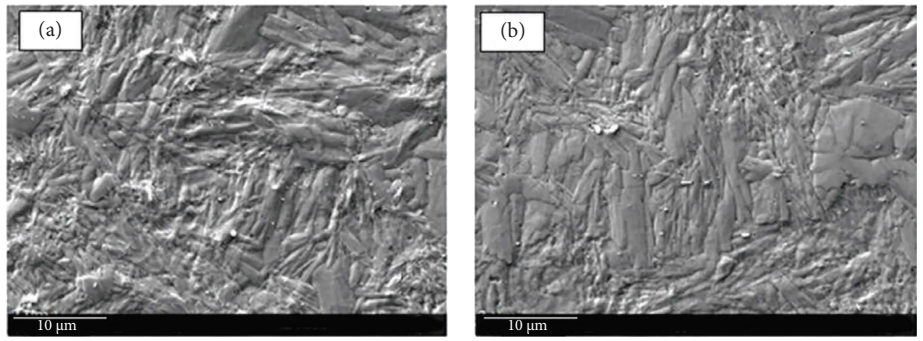

(a) (b)

Figure 6: BD1P and BD3P trained part.

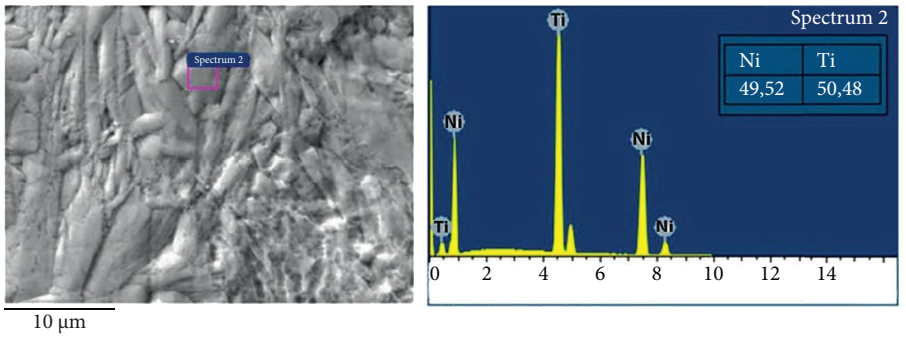

Figure 7: EDX analysis of the sample.

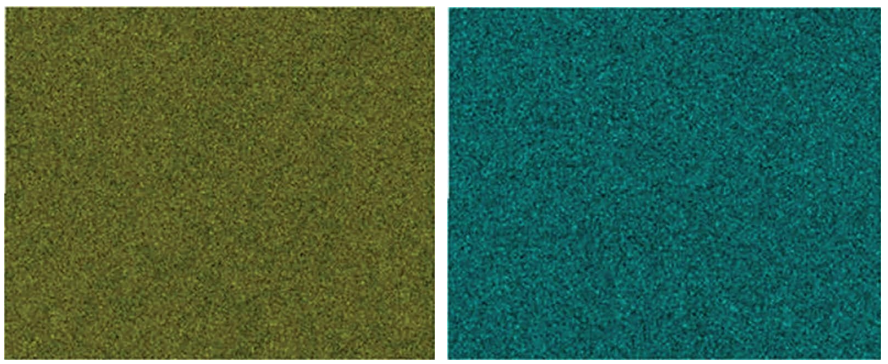

Ti Ni

Figure 8: Homogeneous distribution of Ti and Ni element in the alloy.

driving force contraction during cooling. Additionally, during reverse transformation, the work-hardened dislocations will have contracted. Dislocation causes a spring back force that causes reelongation after the contraction. Primary dislocations cannot produce this kind of force (spring back).

According to Gall et al. [31], the size of Ti3Ni4 precipitants, which are primarily produced during the heat treatment of the strips, is what determines the hardness and resistance to martensite transformation in NiTi alloys. The size of the precipitation also influences the mobility of the dislocations in both the parent and martensite phases, just like it does for regular metals. To be more specific, fine precipitation sizes are distributed properly without the agglomeration phenomenon. The degree of strengthening resulting from the precipitation depends on several factors including the shape, the volume fraction, the average particle diameter, and the interparticle spacing of particles. These factors are all interrelated so that the change of one factor changes the others. When previous authors [32] looked at the relationship between precipitation size and hardness, they discovered that hardness is at its highest when precipitation size is around 10 nm. The hardness decreases as the precipitate size increases to between 100 and 300 nm. According to another study, the critical shear stress for dislocation movement is at its highest when precipitates are

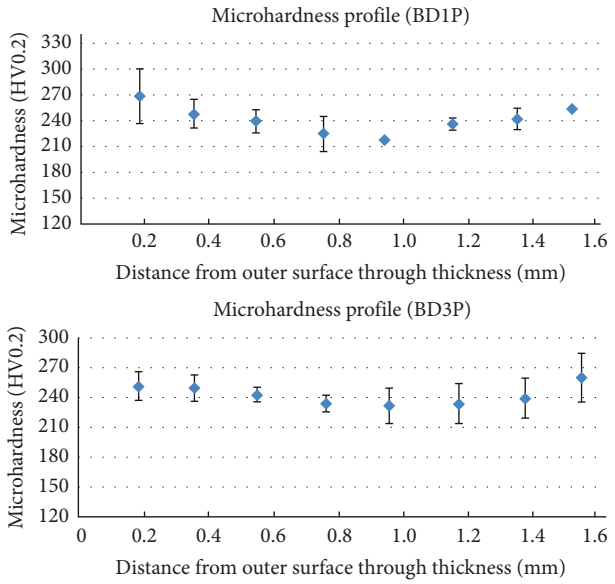

Figure 9: Hardness profiles through thickness for the samples BD1P and BD3P.

around 10 nm in size. When precipitates are 100 nm in size, this value decreases by two times.

3.4. X-Ray Diffraction. Based on X-ray diffraction results, which are shown in Figure 10, there is not so much difference between obtained peaks from as-received strip, BD1P, and BD3P. Austenite and martensite phases have different atomic arrangements. The high-temperature form of nitinol has a body center cubic structure, below the transformation temperature the alloy exists in martensite with lower symmetry. The martensitic form of NiTi alloys can be a monoclinic, triclinic, or distorted hexagonal lattice. Also, just NiTi peaks were detected.

3.5. Training and Two-Way Shape Memory Effect. It should be noted that by applying the bending load to the strip's middle point and to three other points, the effect of the number of deformation points on the two-way strain obtained was investigated (middle and 10 mm distance from both sides of the center). This dimension was taken into account to prevent deformation from interfering with the application of the bending load.

Figure 11 shows how the strips looked in the heating and cooling positions (maximum and minimum deformation of the strips in heating and cooling positions). Additionally, Figure 12 shows the shape of the strips at room temperature.

The data obtained for training strain and two-way strain measurement for BD1P and BD3P are shown in Figures 13 and 14, respectively.

The aforementioned diagrams make it clear that after fifteen to twenty training cycles, the two-way strain in both graphs becomes constant. As seen in Figure 13, the training strain is not constant and stable at the beginning of cycles, which may be due to unevenly applied stress and a higher level of spring back. Due to applying more deformation, the

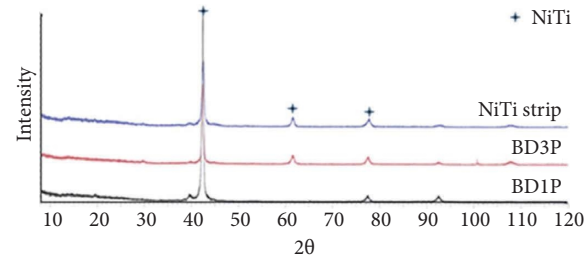

Figure 10: X-ray diffraction for as-received, BD1P, and BD3P samples.

training strain in BD3P was more stable. Additionally, the training strain in BD3P is derived from the initial cycles, whereas in BD1P, the training strain increases over the course of 12 cycles and approaches a two-way strain.

The mean two-way strain in both BD1P and BD3P samples was 3.5%, but BD3P's results were more consistent than BD1P's because the BD1P sample's data in Figure 13 clearly show more variables. Previous researchers [33] looked into how many training cycles had an impact on the two-way shape memory effect. Typically, the two-way strain rises during the initial cycles before leveling off with subsequent cycles. This demonstrated that the training process causes the formation of numerous dislocations, which can result in the creation of a material's oriented stress field and oriented dislocation structure.

As the number of cycles rises, the stress field that is already present stops producing new dislocations. This region, based on an external bending load, leads to preferential martensite deformation. After thermal cycles began, the dislocations consequently interacted with the oriented stress field created by the deformation. This leads to a stable dislocation configuration, which stabilizes the two-way shape memory effect and causes the macroscopic change.

Moreover, the formation of different martensite variances in the outer and inner parts of the strips is what causes the specimen to change shape. In addition, because coherent Ni4Ti3 precipitates are already present in the matrix, a two-way strain is generated. It is necessary to anneal precipitates at a temperature of around 500°C in order to achieve the ideal coherency strain situation. More than this temperature results in larger precipitates and diminished matrix coherency, both of which have a negative impact on the two-way shape memory effect [32]. Worth mentioning is that training-related defects are what cause the two-way shape memory effect. These defects result in residual stress. When the shape memory alloy is cooled without applying load, it then facilitates the formation of preferred martensitic variants. The two-way shape memory effect will be reduced if the residual stress is altered by aging or by adding additional mechanical load [34].

It has been known that the number of dislocations increases with increasing the amount of deformation [35]. Because more dislocations are produced in the BD3P sample, the back transformation to B2 is impeded, the stress field area grows and more stable deformation can be obtained after training. In other words, the increase in dislocation densities is associated with higher driving forces for recrystallization. When dislocation densities increase, driving forces are strong enough to result in

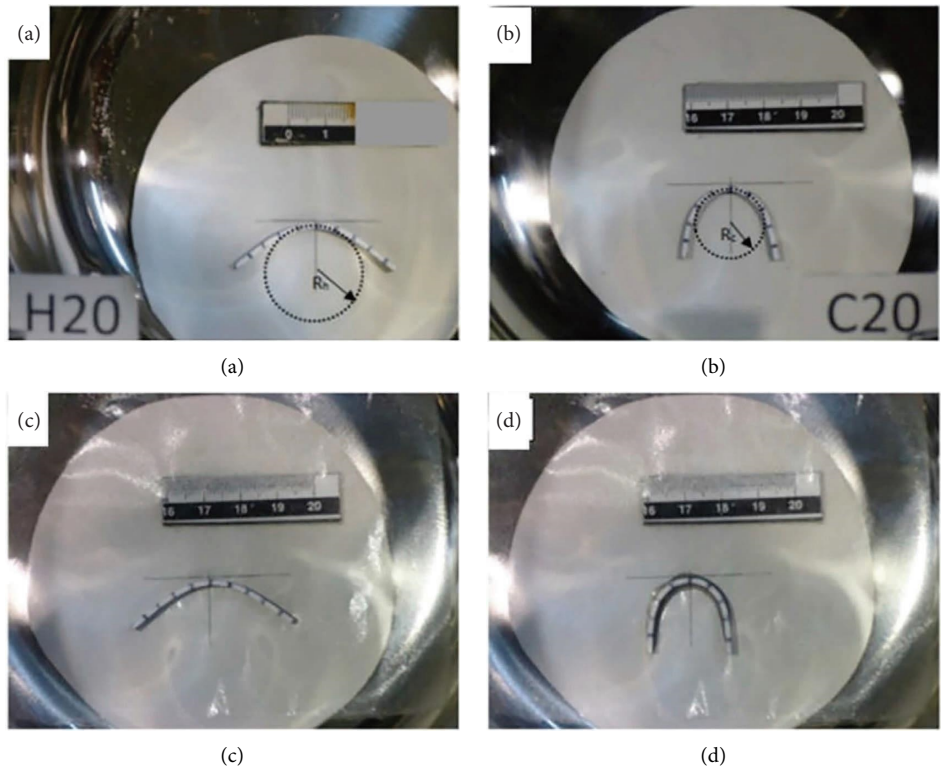

Figure 11: Images of the strip after (a, b) heating and cooling in BD1P and (c, d) heating and cooling in BD3P.

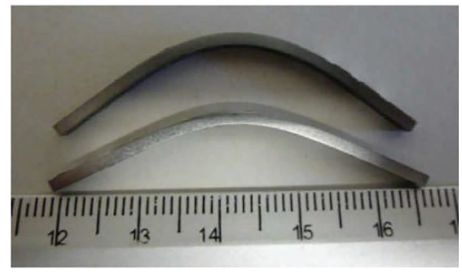

Figure 12: Images of the strips after training at room temperature.

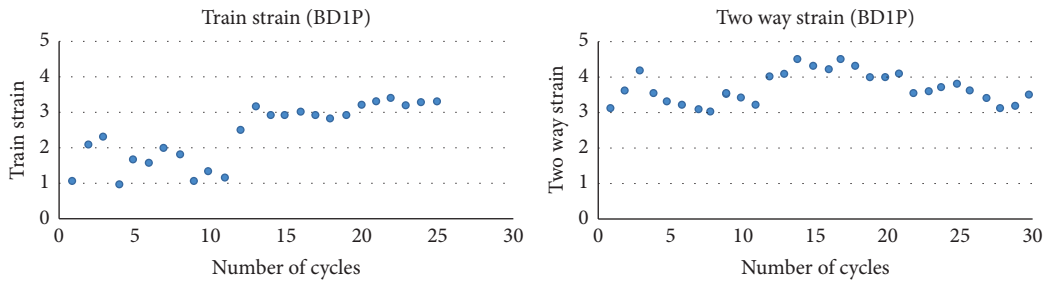

Figure 13: Training strain and two-way strain in the sample BD1P.

complete recrystallization. It should be noted that as deformation increases, M_s and M_f typically increase along with the transformation temperature. The radius of the hot form strip following BD1P deformation was wider than BD3P deformation, which is another problem. Additionally, BD3P's cold form strip was closer than BD1P's. In comparison to the memorized shape stored inside the strip, it can be said that as deformation increases, the rate of elastic spring back decreases and plastic deformation increases. Training with BD1P and BD3P can be carried out depending on the application of the strip that requires more spring back to a memorized shape or a closed circle shape in a cold situation.

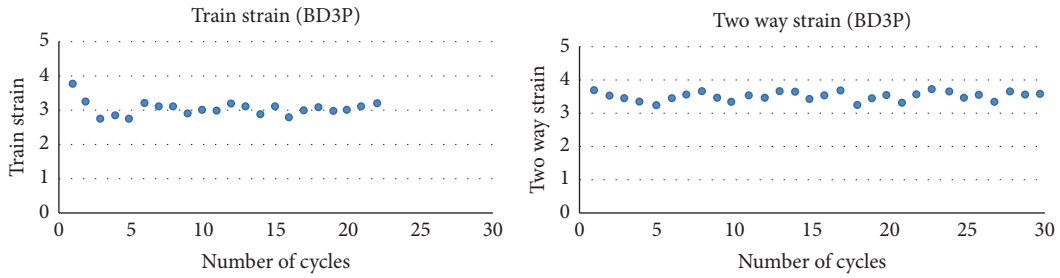

Figure 14: Training strain and two-way strain in BD3P.

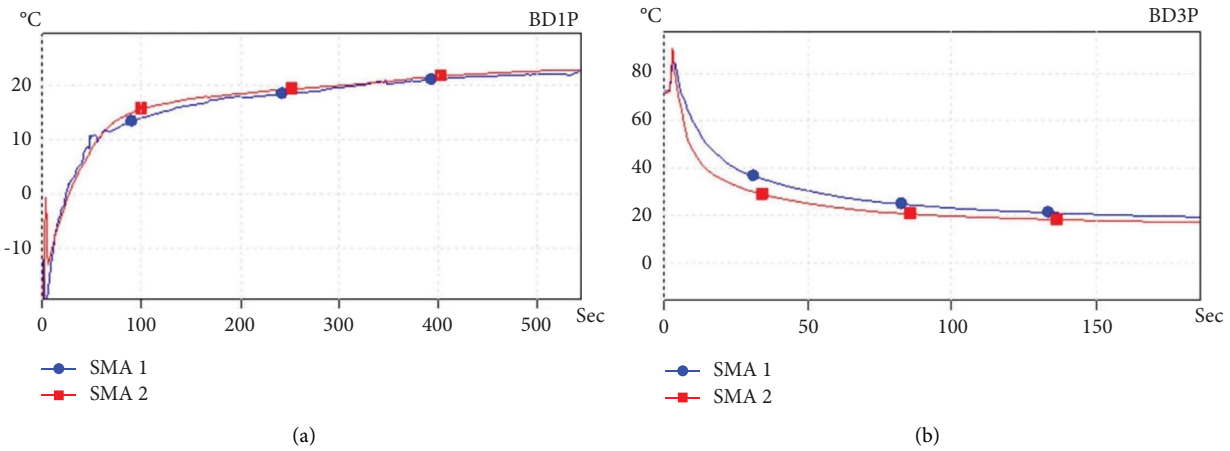

Figure 15: (a) Heating rate from martensite temperature to room temperature for both BD1P and BD3P. (b) Cooling rate from austenite temperature to room temperature for both BD1P and BD3P.

Additionally, Figure 15 depicts the graph for both strips for bringing the temperature of the strip from the temperatures of austenite and martensite to room temperature. As is evident, the temperature becomes constant for heating after 500 seconds and for cooling after 150 seconds. Both strips with one-point and three-point deformation exhibit the same trend of heating and cooling.

Worth mentioning is that the formation of dislocation during training cycles generally results in the two-way strain, which creates a local stress zone and helps the preferred orientation arrangement. Previous studies [7, 36] showed that different training deformations result in different two-way shape memory effect values and that the two-way strain increases as the deformation strain rises. Additionally, with large deformation, training produces more local stress, which is beneficial for producing martensite variants. Consequently, there is a greater production of the two-way shape memory effect. It would be concluded that plastic deformation has a significant impact on the rearrangement of dislocations.

4. Conclusion

This study looked into the effects of various bending positions during the two-way shape memory training process in equiatomic NiTi alloy. The medium value of 3.5% two-way strain can be achieved with bending at one point and three points, but the obtained values for bending at three points were more stable than one-point bending. The results of the average hardness tests for bending at one point and three points were 241 and 247 HV0.2, respectively. According to the strips' hardness profiles, the mean hardness for both strips was the same, but the value at the outer and inner surfaces was higher than at the central points, which is a result of more deformation strain. Less variation in hardness values for BD3P than BD1P may be attributable to a more uniform distribution of deformation throughout the thickness. Based on X-ray diffraction results, there was not so much difference between obtained peaks from as-received strip, BD1P, and BD3P. Depending on how the strip is applied, one-point deformation or three-point deformation can be used to perform more two-way strain or more end close form to a remembered shape, respectively. From thermal analysis, the temperature becomes constant for heating after 500 seconds and for cooling after 150 seconds. Therefore, a predefined thermomechanical procedure is a recommended alternative to precise alloying with the goal of maximizing the indentation-induced TWSME effect within a targeted temperate transformation regime.

Data Availability

Data used to support the findings of this study are available from the corresponding author upon request.

Conflicts of Interest

The authors declare that they have no conflicts of interest.

Acknowledgments

The authors would like to acknowledge Iran's National Elites Foundation.

References

[1] A. I. Tagiltsev, E. Y. Panchenko, Y. I. Chumlyakov, I. D. Fatkullin, and I. Karaman, "Two-way shape memory effect in stress-induced martensite aged Ni50.3Ti32.2Hf17.5 alloy," *Materials Letters*, vol. 268, Article ID 127589, 2020.

[2] K. C. Atli, I. Karaman, R. D. Noebe, and D. Gaydosh, "The effect of training on two-way shape memory effect of binary NiTi and NiTi based ternary high temperature shape memory alloys," *Materials Science and Engineering: A*, vol. 560, pp. 653–666, 2013.

[3] J. Mohd Jani, M. Leary, A. Subic, and M. A. Gibson, "A review of shape memory alloy research, applications and opportunities," *Materials and Design*, vol. 56, pp. 1078–1113, 2014.

[4] C. M. Laursen, N. J. Peter, G. Gerstein, H. J. Maier, G. Dehm, and C. P. Frick, "Influence of Ti3Ni4 precipitates on the indentation-induced two-way shape-memory effect in Nickel-Titanium," *Materials Science and Engineering: A*, vol. 792, Article ID 139373, 2020.

[5] V. Torra, F. Martorell, F. C. Lovey, and M. L. Sade, "Civil engineering applications: specific properties of NiTi thick wires and their damping capabilities, A review," *Shape Memory and Superelasticity*, vol. 3, no. 4, pp. 403–413, 2017.

[6] W. Li, Z. X. Zhou, H. Xiao, X. M. Huang, and Y. Q. Luo, "Effects of annealing and training on NiTi alloy ring for clamping device," *Materials and Manufacturing Processes*, vol. 31, no. 15, pp. 2011–2016, 2016.

[7] Z. Balak and S. M. Abbasi, "Influence of the Ti content, training cycles and pre-strain on the two-way shape memory effect in NiTi alloys," *Materials & Design*, vol. 32, no. 7, pp. 3992–3996, 2011.

[8] T. W. Duerig, K. N. Melton, D. Stockel, and C. M. ayman, *Engineering Aspect of Shape Memory Alloys*, Butterworth-Heinmann Ltd, Oxford, UK, 1990.

[9] I. Ponikarova, S. Belyaev, and N. Resnina, "Degradation of two-way shape memory effect due to the relaxation of internal oriented stress in NiTi alloy on holding at 640÷700 K," *Mechanics of Materials*, vol. 138, Article ID 103174, 2019.

[10] L. Xu, A. Solomou, T. Baxevanis, and D. Lagoudas, "Finite strain constitutive modeling for shape memory alloys considering transformation-induced plasticity and two-way shape memory effect," *International Journal of Solids and Structures*, vol. 221, pp. 42–59, 2021.

[11] I. Rita, K. Babicheva, and Y. Mulyukov, "Thermomechanical treatment to achieve stable two-way shape memory strain without training in Ti-49.8 at.% Ni alloy," *Applied Physics A*, vol. 116, 2014.

[12] F. S. Beliaev, M. E. Evard, E. S. Ostropiko, A. I. Razov, and A. E. Volkov, "Aging effect on the one-way and two-way shape memory in TiNi-based alloys," *Shap. Mem. Superelasticity*, vol. 5, no. 3, pp. 218–229, 2019.

[13] E. S. Ostropiko and A. I. Razov, "The influence of long-term storage on the functional properties of shape memory alloys," *Experimental Mechanics*, vol. 58, no. 8, pp. 1305–1310, 2018.

[14] M. Kök, H. S. A. Zardawi, I. N. Qader, and M. Sait Kanca, "The effects of cobalt elements addition on Ti2Ni phases, thermodynamics parameters, crystal structure and transformation temperature of NiTi shape memory alloys," *European Physical Journal E: Soft Matter*, vol. 134, no. 5, p. 197, 2019.

[15] Y. N. Zhao, S. Y. Jiang, Y. Q. Zhang, and Y. L. Liang, "Influence of Fe addition on phase transformation, microstructure and mechanical property of equiatomic NiTi shape memory alloy," *Acta Metallurgica Sinica*, vol. 30, no. 8, pp. 762–770, 2017.

[16] M. Kök and G. Ateş, "The effect of addition of various elements on properties of NiTi-based shape memory alloys for biomedical application," *European Physical Journal E: Soft Matter*, vol. 132, no. 4, p. 185, 2017.

[17] S. Waqar, A. Wadood, A. Mateen, and M. A. U. Rehman, "Effects of Ni and Cr addition on the wear performance of NiTi alloy," *International Journal of Advanced Manufacturing Technology*, vol. 108, no. 3, pp. 625–634, 2020.

[18] I. N. Qader, E. Ercan, and A. Orhan, "Effect of boron element additions on microstructure, biocompatibility, and thermodynamic parameters of NiTi shape memory alloy," *Journal of the Minerals Metals & Materials Society*, vol. 74, no. 11, pp. 4402–4409, 2022.

[19] F. Dagdelen, M. Kok, and I. N. Qader, "Effects of Ta content on thermodynamic properties and transformation temperatures of shape memory NiTi alloy," *Metals and Materials International*, vol. 25, no. 6, pp. 1420–1427, 2019.

[20] J. Li, X. Yi, K. Sun et al., "The effect of Zr on the transformation behaviors, microstructure and the mechanical properties of Ti-Ni-Cu shape memory alloys," *Journal of Alloys and Compounds*, vol. 747, pp. 348–353, 2018.

[21] R. Rizzoni, M. Merlin, and D. Casari, "Shape recovery behaviour of NiTi strips in bending: experiments and modelling," *Continuum Mechanics and Thermodynamics*, vol. 25, no. 2-4, pp. 207–227, 2013.

[22] K. W. K. Yeung, K. M. C. Cheung, W. W. Lu, and C. Y. Chung, "Optimization of thermal treatment parameters to alter austenitic phase transition temperature of NiTi alloy for medical implant," *Materials Science and Engineering A*, vol. 383, no. 2, pp. 213–218, 2004.

[23] I. Kaya, E. Acar, and H. E. Karaca, "Effects of deformation temperature and amount on the two-way shape memory effect of solutionized Ni50.8Ti49.2 alloys," *Intermetallics*, vol. 114, Article ID 106607, 2019.

[24] P. Rasmussen, R. Berlia, R. Sarkar, and J. Rajagopalan, "Mechanical behavior of nanocrystalline and ultrafine-grained NiTi thin films," *Materialia*, vol. 15, Article ID 100994, 2021.

[25] M. Xia, P. Liu, and Q. Sun, "Grain size dependence of Young's modulus and hardness for nanocrystalline NiTi shape memory alloy," *Materials Letters*, vol. 211, pp. 352–355, 2018.

[26] Y. Sun, J. Luo, and J. Zhu, "Phase field study of the microstructure evolution and thermomechanical properties of polycrystalline shape memory alloys: grain size effect and rate effect," *Computational Materials Science*, vol. 145, pp. 252–262, 2018.

[27] N. Resnina, S. Belyaev, V. Zeldovich, V. Pilyugin, N. Frolova, and D. Glazova, "Variations in martensitic transformation parameters due to grains evolution during post-deformation heating of Ti-50.2 at% Ni alloy amorphized by HPT," *Thermochimica Acta*, vol. 627–629, pp. 20–30, 2016.

[28] B. Xu, C. Yu, and G. Kang, "Phase field study on the microscopic mechanism of grain size dependent cyclic degradation of super-elasticity and shape memory effect in nano-

polycrystalline NiTi alloys," *International Journal of Plasticity*, vol. 145, Article ID 103075, 2021.

[29] A. Amini and C. Cheng, "Scientific Reports," *Nature*, vol. 3, no. 2476, pp. 1–6, 2013.

[30] A. L. Gloanec, G. Bilotta, and M. Gerland, "Deformation mechanisms in a TiNi shape memory alloy during cyclic loading," *Materials Science and Engineering: A*, vol. 564, pp. 351–358, 2013.

[31] K. Gall, K. Juntunen, H. J. Maier, H. Sehitoglu, and Y. I. Chumlyakov, "nstrumented micro-indentation of NiTi shape-memory alloys," *Acta Materialia*, vol. 49, pp. 3205–3217, 2001.

[32] M. S. Shakeri, J. Khalil-Allafi, V. Abbasi-Chianeh, and A. Ghabchi, "The influence of Ni4Ti3 precipitates orientation on two-way shape memory effect in a Ni-rich NiTi alloy," *Journal of Alloys and Compounds*, vol. 485, no. 1-2, pp. 320–323, 2009.

[33] X. L. Meng, Y. F. Zheng, W. Cai, and L. C. Zhao, "Two-way shape memory effect of a TiNiHf high temperature shape memory alloy," *Journal of Alloys and Compounds*, vol. 372, no. 1-2, pp. 180–186, 2004.

[34] M. Mohri and M. Nili-Ahmadabadi, "Phase transformation and structure of functionally gradedNi–Ti bi-layer thin films with two-way shape memory effect," *Sensors and Actuators A: Physical*, vol. 228, pp. 151–158, 2015.

[35] J. Burow, J. Frenzel, C. Somsen, E. Prokofiev, R. Valiev, and G. Eggeler, "Grain nucleation and growth in deformed NiTi shape memory alloys: an in situ TEM study," *Shap. Mem. Superelasticity*, vol. 3, no. 4, pp. 347–360, 2017.

[36] J. S. Owusu-Danquah, A. F. Saleeb, and M. A. Soudah, "Cyclic pseudoelastic training and two-way shape memory behavior of a NiTi alloy with small irrecoverable plastic strains:numerical modeling," *International Journal of Solids and Structures*, vol. 217-218, pp. 178–192, 2021.